

# Determining a Perturbation Factor to Design Tunable Resonant Cavities in SIW Technology

Ricardo Caranicola Caleffo , Fatima Salete Correra 

Department of Electronic Systems Engineering, School of Engineering/ Polytechnic School, University of São Paulo, São Paulo, 05508-970, Brazil  
[ricardocaleffo@alumni.usp.br](mailto:ricardocaleffo@alumni.usp.br), [fcorrera@usp.br](mailto:fcorrera@usp.br)

**Abstract** — This paper presents an effective and novel design procedure employing a novelty named as Perturbation Factor to predict the resonance frequency of resonant cavities in SIW technology perturbed by a shape perturbation. The design procedure can be applied in tunable cavities and bandpass filters with shunt reactance of symmetrical inductive window, and regarding the application technologies, rectangular waveguide resonators and resonant cavities in SIW can be employed due to the equivalence of operation between both technologies. Its straightforward application allows a frequency variation of up to 20% using only one metal post which allows the reduction of the fabrication cost and the preservation of the frequency response across the considered bandwidth. To validate the design procedure, two resonant cavities were fabricated, a rectangular resonant cavity designed to operate at 5.0 GHz and 6.0 GHz and a square resonant cavity designed to operate at 6.0 GHz and 7.2 GHz, and frequency variations of 17.74% and 21.81% were obtained for the rectangular and square cavities, respectively. Still regarding the reached results, was verified a mean error of 1.75% for the predicted resonance frequency, which validates the design procedure. The experimental results are in good agreement with the full-wave computational results and electromagnetic theory.

**Index Terms**— Perturbation theory, Resonance frequency, Shape perturbations, Substrate Integrated Waveguide, Tunable resonant cavities.

## I. INTRODUCTION

Nowadays, the needs exposed by the recent technological trends are stimulating the development of new ways and concepts of structures operating from lower frequencies to higher frequencies, changing profoundly people's lives. Therefore, an idea comes to our mind; the pursuit of higher-performance communication systems is never-ending. In this context, the Fifth Generation (5G) technology is being widely explored and applied worldwide to improve the performance and capacity of communication systems to be used in Industry 4.0 and its smart manufacturing, Internet of Things (IoT), and mobile communication.

The 5G aims to improve the transmission capacity data, broadcasting multiple and simultaneous links, and support Multiple Inputs and Multiple Outputs (MIMO) systems. Regarding its implementation, the global situation of spectrum for 5G technology can be divided into two spectrums: below 6 GHz and above 6 GHz. Various countries and regions from South America, North America,

Europe, and Asia, are giving special attention to the spectrum below 6 GHz, the range from 3.3 GHz to 4.2 GHz and the 4.4 GHz to 5.0 GHz, and above 6 GHz, the range from 24 GHz to 29.5 GHz and the 37.0 GHz to 40.0 GHz. Various bands below 1 GHz and some existing LTE bands are also included in this scenario [1]. The microwave circuits to be used in the 5G Base Station, referred as gNodeB, need to operate at more than one frequency, as just mentioned earlier, and tunable bandwidth: (a) 100 MHz of maximum cell bandwidth for frequencies below 6 GHz; and (b) 400 MHz of maximum cell bandwidth for frequencies higher than 24 GHz. [2] The bandwidths for frequencies below 6 GHz are: 5 MHz, 10 MHz, 15 MHz, 20 MHz, 25 MHz, 30 MHz, 40 MHz, 50 MHz, 60 MHz, 70 MHz, 80 MHz, 90 MHz, and 100 MHz, and the bandwidths for frequencies higher than 24 GHz are: 50 MHz, 100 MHz, 200 MHz, and 400 MHz. With all these requirements for frequency operation and bandwidth, reliable and low losses tunable microwave circuits are crucial to meet this demand. This is the driving force of the proposed work.

This new technological moment requires the development of versatile and tunable microwave circuits, allowing high-frequency structures to operate at more than one frequency or band. To meet this presented demand, the Substrate Integrated Waveguide (SIW) technology [3]-[8], or simply SIW technology, can be employed to design planar circuits in the microwave spectrum due to its straightforward integration with several planar circuits, low-cost fabrication, and high applicability [3]-[4], allowing the development of liquid characterization sensors [9], tunable resonant cavities [10]-[11], tunable bandpass filters [12]-[15],[20], and split-ring resonators [21].

Aiming to contribute to the current scientific and technological moment, this paper proposes a novel design procedure, employing a novelty developed in this work and named as Perturbation Factor (PF) during the investigation, to predict the resonance frequency of resonant cavities in SIW technology perturbed by a single metal post inserted in its internal volume, connecting the bottom and upper metal walls. The proposed design procedure is the first scientific work that considers the position variation and the physical dimensions of the metal post. Regarding its applications, two resonant cavities in SIW technology, a rectangular cavity and a square cavity, perturbed by a single metal post each of them, were designed employing the novel design procedure and their frequency variations were verified by electromagnetic simulation and experimental characterization. The rectangular resonant cavity operates at 5.0 GHz and 6.0 GHz and the square resonant cavity operates at 6.0 GHz and 7.2 GHz.

In the reminder, Section 2 describes the proposed design procedure, Section 3 shows the fabricated resonant cavities and experimental results, and finally, Section 4 presents the conclusions.

## II. PREDICTING THE RESONANCE FREQUENCIES OF PERTURBED RESONANT CAVITIES IN SIW TECHNOLOGY

Resonant cavities are often modified by making changes in their size or by inserting a metal post through its internal volume, connecting the bottom and upper walls. These modifications are

considered shape perturbations and they are responsible for varying the resonance frequency [16]-[17],[19],[22], operating frequency. This section presents a novel design procedure and expression for the resonance frequency, as a function of the position of the metal post, when a resonant cavity in SIW technology is perturbed by a change in its shape, a single metal post inserted in its internal volume and permanently connected at the bottom and upper walls. To obtain an expression for the resonance frequency of an arbitrary cavity in SIW technology perturbed by a metal post connecting its bottom and upper walls, let us consider Fig. 1.

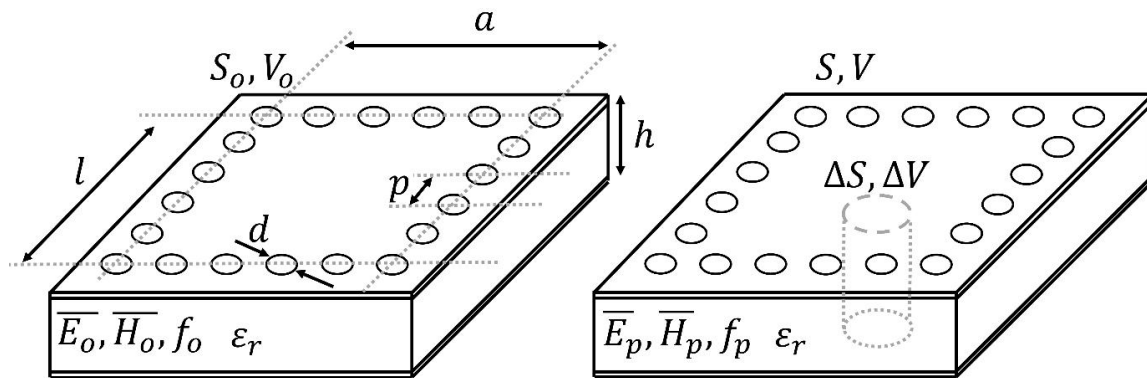


Fig.1. An original resonant cavity in SIW technology (on the left) and the same cavity perturbed by a metal post (on the right).

According to Fig. 1,  $\overline{E}_o$  and  $\overline{H}_o$  are the electric and magnetic fields, respectively, and  $f_o$  is the resonance frequency of the original cavity, and  $\overline{E}_p$  and  $\overline{H}_p$  are the electric and magnetic fields, respectively, and  $f_p$  is the resonance frequency of the perturbed cavity. The original cavity has a volume  $V_o$  and surface  $S_o$  and the perturbed cavity has a volume  $V$  and surface  $S$ ; the metal post has a volume  $\Delta V = V_o - V$  and surface  $\Delta S = S_o - S$ . Its physical dimensions are the width  $a$ , diameter of the metal vias, copper conductors, that compose the SIW sidewalls  $d$ , length  $l$ , longitudinal spacing  $p$ , and height  $h$ . The dielectric substrate is considered lossless with a dielectric constant  $\epsilon_r$  and nonmagnetic with relative permeability ( $\mu_r$ ) equal to unity, a purely lossless dielectric material. Assuming harmonic fields, then Maxwell's curl equations [16]-[18] in the phasor form for both cases can be written as

$$\nabla \times \overline{E}_o = -j\omega_o \mu_r \mu_o \overline{H}_o \quad | \quad \mu_r = 1, \quad (1)$$

$$\nabla \times \overline{H}_o = j\omega_o \epsilon_r \epsilon_o \overline{E}_o, \quad (2)$$

$$\nabla \times \overline{E}_p = -j\omega_p \mu_r \mu_o \overline{H}_p \quad | \quad \mu_r = 1, \quad (3)$$

$$\nabla \times \overline{H}_p = j\omega_p \epsilon_r \epsilon_o \overline{E}_p, \quad (4)$$

where  $\omega = 2\pi f$  is the radian frequency. Reference [16] shows the mathematical procedure to obtain an exact expression for the new resonance frequency, related to a resonant cavity perturbed by shape perturbation, as follows

$$f_p = \frac{-j \oint_{\Delta S} (\overline{E}_o^* \times \overline{H}_p) \cdot d\overline{S}}{2\pi \iiint_V [\epsilon_r \epsilon_o (\overline{E}_p \cdot \overline{E}_o^*) + \mu_o (\overline{H}_p \cdot \overline{H}_o^*)] dv} + f_o. \quad (5)$$

However, (5) is not particularly useful since it is hard to find expressions for  $\overline{E}_p$  and  $\overline{H}_p$ . Normally, we only have  $\overline{E}_o$  and  $\overline{H}_o$ . For weakly perturbed cavities,  $\overline{E}_p \approx \overline{E}_o$  and  $\overline{H}_p \approx \overline{H}_o$  (Perturbation Method [16]-[17]), and assuming  $\Delta S$  is small, it is possible to obtain an expression for the approximate fractional change in resonance frequency as [16]-[17]:

$$f_p \approx f_o \left[ \frac{\iiint_{\Delta V} (\mu_o |\overline{H}_o|^2 - \epsilon_r \epsilon_o |\overline{E}_o|^2) dv}{\iiint_{V_o} (\epsilon_r \epsilon_o |\overline{E}_o|^2 + \mu_o |\overline{H}_o|^2) dv} + 1 \right] = f_o \left[ \frac{\Delta W_m - \Delta W_e}{W_m + W_e} + 1 \right], \quad (6)$$

where  $\Delta W_m$  is the magnetic energy removed,  $\Delta W_e$  the electric energy removed, and  $W_m + W_e$  the total stored energy. Equation (6) shows that a shape perturbation affects the stored energy and causes a shift in the resonance frequency. It is important to cite that in the condition of resonance, the stored magnetic and electric energies are equal. If a shape perturbation is made, such as a metal post connecting upper and bottom walls, this will change one type of energy more than the other, for this case, the resonance frequency would then shift to again equalize the energies. Equation (6) cannot be applied in strongly perturbed cavities,  $\overline{E}_p \neq \overline{E}_o$  and  $\overline{H}_p \neq \overline{H}_o$ , however, it is useful to explain the phenomenon of resonance frequency variation ( $\Delta f$ ) in resonant cavities perturbed by shape perturbations. For a metal post connecting the bottom and upper walls, imposing the boundary condition  $\hat{n} \times \overline{E} = 0$  at the location and shifting the maximum electric field, there is an increase of the magnetic energy caused by the flow of a current density ( $\overline{J}$ ) through its metal structure.

In general, to obtain an exact value for  $f_p$  in strongly perturbed cavities using (5), it is crucial knowing expressions for  $\overline{E}_p$  and  $\overline{H}_p$ , and to get it, it is necessary to use Maxwell's equations, correctly apply the boundary conditions, and consider the position and physical dimension of the metal post in the investigation. Normally, this is a challenging task to perform. Aiming to make it easier, computational simulators, such as the High Frequency Structure Simulator (HFSS), has been widely used to obtain the field distributions in complex structures operating in the microwave spectrum.

Related to HFSS, there is a valuable tool named Fields Calculator that allows solving equations and expressions from the field distributions of complex structures without performing approximations. The Fields Calculator was used during this investigation to obtain the Perturbation Factor (PF), a novelty developed in this work, aiming to predict the resonance frequency of resonant cavities in SIW technology perturbed by a single metal post inserted in its internal volume, connecting the bottom and upper metal walls. In order to present the PF, let us consider a resonant cavity perturbed by a single metal post, as shown in Fig. 2.

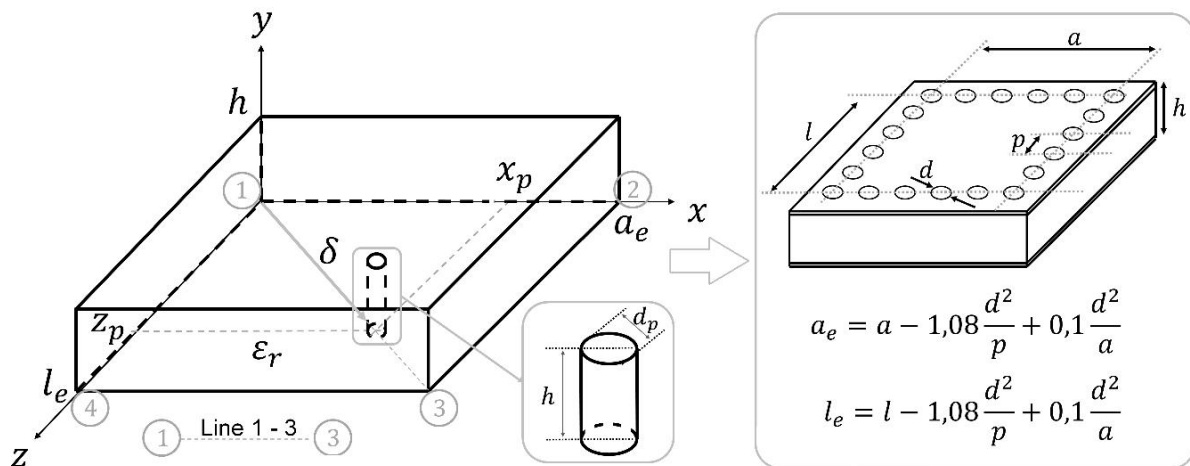


Fig.2. A resonant cavity in SIW technology perturbed by a metal post having its position varied along Line 1 – 3.

In this case, the dielectric substrate has a thickness  $h$  and a dielectric constant  $\epsilon_r$ ,  $x_p$  and  $z_p$  are the metal post position, and  $a_e$  is the effective width and  $l_e$  is the effective length of an ordinary resonant cavity in SIW technology [3]-[8]. To obtain the PF, it is being considered that the original cavity, the unperturbed cavity, operates in TE<sub>101</sub> mode and the metal post is moved along Line 1–3 or Line 2–4, due to its symmetry, in the perturbed cavity, allowing to rewrite (5) as

$$f_p = \frac{-j \oint_{\Delta S} (\vec{E}_o^* \times \vec{H}_p) \cdot d\vec{S}}{2\pi \iiint_V [\epsilon_r \epsilon_o (\vec{E}_p \cdot \vec{E}_o^*) + \mu_o (\vec{H}_p \cdot \vec{H}_o^*)] dv} + \frac{c}{2\sqrt{\epsilon_r}} \sqrt{\frac{1}{a_e^2} + \frac{1}{l_e^2}}, \quad (7)$$

where  $c$  is the speed of light in free-space, and defining the normalized distance  $\delta$ , see Fig. 2, as

$$\delta = \sqrt{\frac{x_p^2 + z_p^2}{a_e^2 + l_e^2}}, \text{ for } 0 \leq \delta \leq 1. \quad (8)$$

The first term on the right side of (7) will be written as a multiple of the second term, as follows

$$PF(\delta) = \frac{\left( \frac{-j \oint_{\Delta S} (\vec{E}_o^* \times \vec{H}_p) \cdot d\vec{S}}{2\pi \iiint_V [\epsilon_r \epsilon_o (\vec{E}_p \cdot \vec{E}_o^*) + \mu_o (\vec{H}_p \cdot \vec{H}_o^*)] dv} \right)}{\frac{c}{2\sqrt{\epsilon_r}} \sqrt{\frac{1}{a_e^2} + \frac{1}{l_e^2}}}. \quad (9)$$

The  $PF(\delta)$  is named as Perturbation Factor and depends on the fields of the original and perturbed cavity, the resonance frequency of the original cavity, and the dielectric constant. According to (9), if  $PF(\delta) = 0$  then  $f_p = f_o$ ,  $PF(\delta) > 0$  then  $f_p > f_o$ , and  $PF(\delta) < 0$  then  $f_p < f_o$ .

Aiming to fully understand the behavior of the PF, seven resonant cavities were designed on a RT/duroid 5880 and a RO4003C, being three square cavities and four rectangular cavities, in SIW technology perturbed by a single metal post each one of them. Fig. 3 shows the Seven-Step Procedure (SSP), a procedure developed in this work to obtain values for the PF.

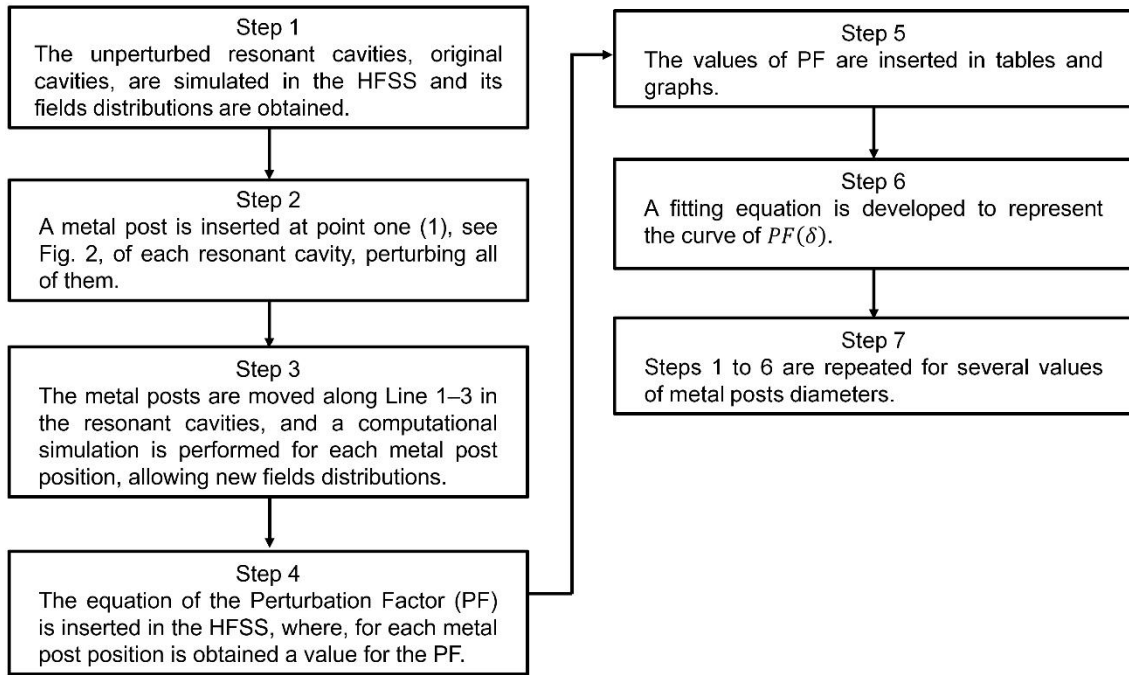


Fig. 3. Flowchart of the Seven-Step Procedure (SSP).

After performing the SSP several times to obtain values for the PF, was observed a relation involving the metal post diameter and physical dimensions of the resonant cavity, such relation is named in this work as Perturbation Factor Rule (PFR), allowing a common PF for all the seven designed cavities. The PFR can be written as

$$a > l \rightarrow \frac{d_p}{a} = 0.03, \quad (10)$$

$$l > a \rightarrow \frac{d_p}{l} = 0.03, \quad (11)$$

$$a = l \rightarrow \frac{d_p}{a} = \frac{d_p}{l} = 0.03, \quad (12)$$

where  $a$  is the width and  $l$  is the length of the SIW cavity. In other words, the PFR says that the  $d_p$  must be 3% of the larger physical dimension of the resonant cavity. Fig. 4(a) shows the  $PF(\delta)$  considering the SSP and PFR.

In summary, Fig. 4(a) shows that the resonant cavity is strongly perturbed for a metal post located at its center,  $\delta = 0.50$ . For a metal post located close to the sidewalls,  $\delta = 0$  or  $\delta = 1$ , the cavity is weakly perturbed and the PF is minimum, approximately zero. Furthermore, considering the PFR, the  $f_p$  can be increased up to 20% of  $f_o$ . For comparative purposes, [10] predicts a perturbed resonance frequency of 18% of  $f_o$  for a metal post with a diameter of 1.00 mm located at the center of a square cavity.



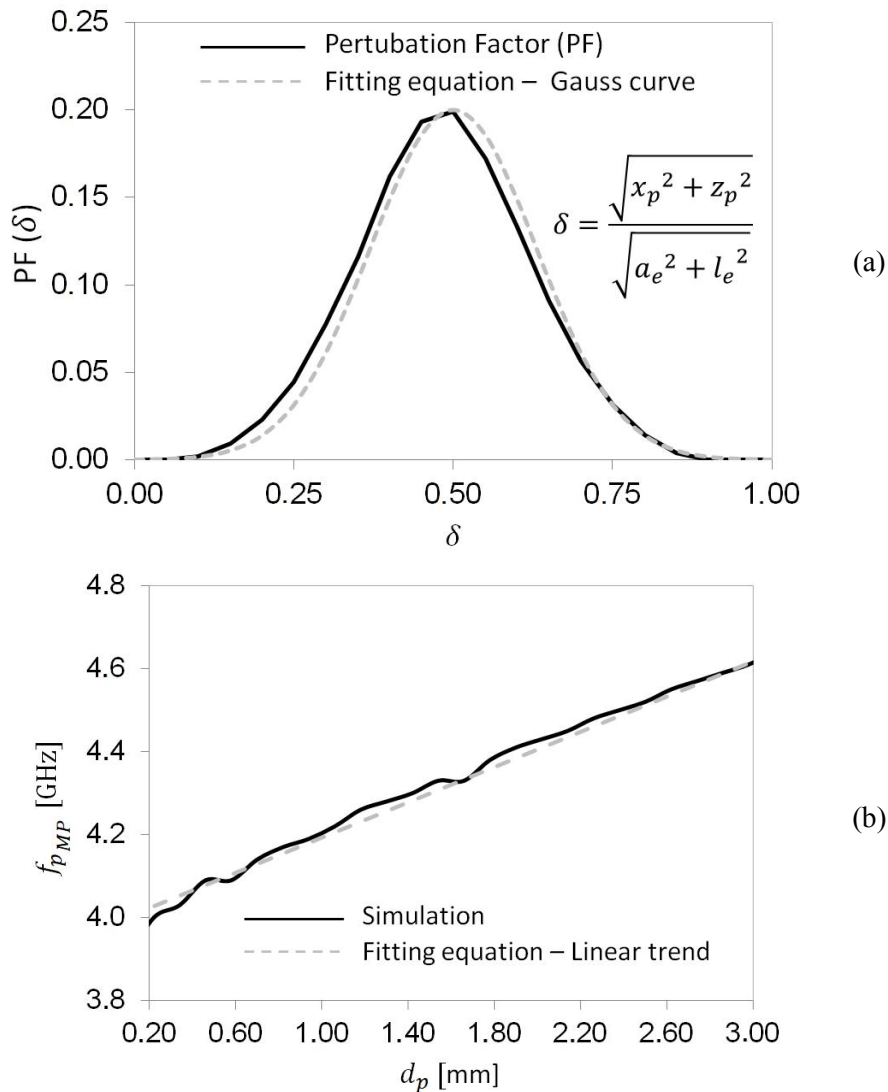


Fig. 4. (a) The graph of the  $PF(\delta)$  and (b) The graph of the  $f_{p_{MP}}(d_p)$ , in this case, is considered the resonant cavity on the condition of maximum perturbation, or  $\delta = 0.50$ .

The obtained values for the PF are in good agreement with the field distributions and the boundary conditions imposed by the resonant cavity structure. For the original cavity operating in the  $TE_{101}$  mode, the electric field is maximum at its center and minimum close to the sidewalls; and for the perturbed cavity, the metal post imposes  $\hat{n} \times \vec{E} = 0$ , shifting the transverse electric field, letting its distribution with a “donut” shape, and changing the stored magnetic and electric energies, see Fig. 5. Thus, there is an increase of the magnetic energy caused by the flow of a current density through the perturbation structure.

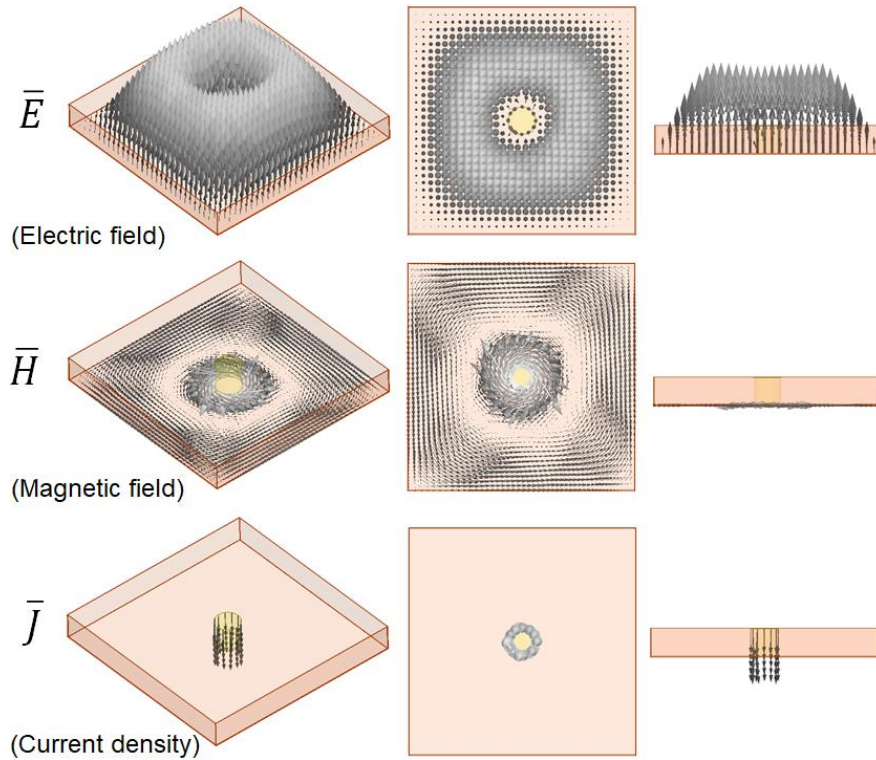


Fig. 5. Field distributions of a resonant cavity in SIW technology perturbed by a metal post through its internal volume, connecting the bottom and upper walls.

According to Fig. 4(a), it is possible to apply a Gauss curve, dashed line, to obtain a fitting equation to represent the  $PF(\delta)$ , solid line, making it possible to write

$$PF(\delta) = 0.20e^{-\left(\frac{\delta-0.50}{0.13\sqrt{2}}\right)^2} = \frac{1}{5}e^{-\left(\frac{100\delta-50}{13\sqrt{2}}\right)^2}. \quad (13)$$

Therefore, applying (9) and (13) to (7) gives

$$f_p(\delta) = \left[ \frac{1}{5}e^{-\left(\frac{100\delta-50}{13\sqrt{2}}\right)^2} + 1 \right] \frac{c}{2\sqrt{\epsilon_r}} \sqrt{\frac{1}{a_e^2} + \frac{1}{l_e^2}}. \quad (14)$$

Equation (14) is strictly valid for the metal post being moved along Line 1–3, or Line 2–4 due to the symmetry, original cavity operating in  $TE_{101}$  mode, and using the PFR. It is important to cite that (14) can be applied and used in rectangular waveguide resonators and resonant cavities in SIW technology due to the equivalence of operation between both technologies. According to the performed investigation, it was verified that the resonant cavity in SIW technology is strongly perturbed by a metal post having its position varied. Moreover, the diameter of the metal post also influences the operation of the perturbed resonant cavity. So far it has been considered a fixed value for  $d_p$ , 3% of the larger physical dimension of the resonant cavity, according to the PFR, however, it is straightforward to verify that other values also perturb and influence the operation of resonant cavities.

Aiming to fully understand the influence of the diameter of the metal post in perturbed resonant cavities, various electromagnetic simulations were performed to comprehend how the resonance



frequency varies as a function of the diameter of the metal post. The electromagnetic simulations consider a resonant cavity in SIW technology designed on a RO4003C with a thickness of 0.635 mm, width  $a$  and length  $l$  of 33.2 mm, longitudinal spacing  $p$  of 2.54 mm, diameter  $d$  of the metal vias that compose the SIW sidewalls of 1.00 mm, and maximum perturbation ( $\delta = 0.50$ ). The diameter of the metal post varies from 0.60% up to 9.04% of the larger physical dimension of the resonant cavity, corresponding to diameters ranging from 0.20 mm up to 3.00 mm, respectively. Fig. 4(b) shows a solid line, simulation results, related to  $f_p$  for  $\delta = 0.50$ ,  $f_{p_{MP}}$  [GHz], as a function of  $d_p$  [mm], giving the linear trend, dashed line,

$$f_{p_{MP}}(d_p) = 0.2121d_p + 3.9815 \text{ [GHz]}, \quad (15)$$

with Pearson Correlation Coefficient ( $R^2$ ) of 0.9908. The resonance frequency varies from 94,5% up to 110% of 4.19 GHz, where 4.19 GHz is the resonance frequency related to the diameter of 1.00 mm of the metal post given by PFR. Concerning the frequency of 4.1936 GHz, a key point to observe is an error of 1.7% for  $d_p$  of 1.00 mm, given by the PFR. Equation (14) predicts a resonance frequency of 4.12 GHz, demonstrating its effectiveness.

It is important to note that thin metal posts are not capable of strongly perturbing the field distributions, in contrast, thick metal posts change the original structure of the resonant cavity. Furthermore, diameters of the metal post smaller than 0.60% and bigger than 9.00%, considering the larger physical dimension, create difficulties for manufacturing and should be avoided. Another approach to increase the perturbation is using various metal posts inside the cavity structure [11],[13]-[15], but for this approach, there is no equation to predict the perturbed resonance frequency as a function of the metal posts' location.

### III. RESONANT CAVITIES FABRICATION AND EXPERIMENTAL RESULTS

Regarding its applications, two resonant cavities in SIW technology, a rectangular cavity and a square cavity, perturbed by a single metal post each of them, were designed on a RT/duroid 5880 with a thickness of 0.508 mm employing the novel design procedure and then fabricated. Their performances were verified computationally, using the HFSS, and experimentally. A Vector Network Analyzer HP8722 was used to perform the electrical characterization. The rectangular resonant cavity was designed to operate at 5.0 GHz and 6.0 GHz, and the square resonant cavity was designed to operate at 6.0 GHz and 7.2 GHz; the lower resonance frequency is  $f_o$  and the higher resonance frequency is  $f_p$  for  $\delta = 0.50$  and considering the PFR, (14). Fig. 6(a) and Fig. 6(b) show photographs of the fabricated rectangular cavity and square cavity, respectively, and Fig. 6(c) shows the measurement setup used to perform the electrical characterization.

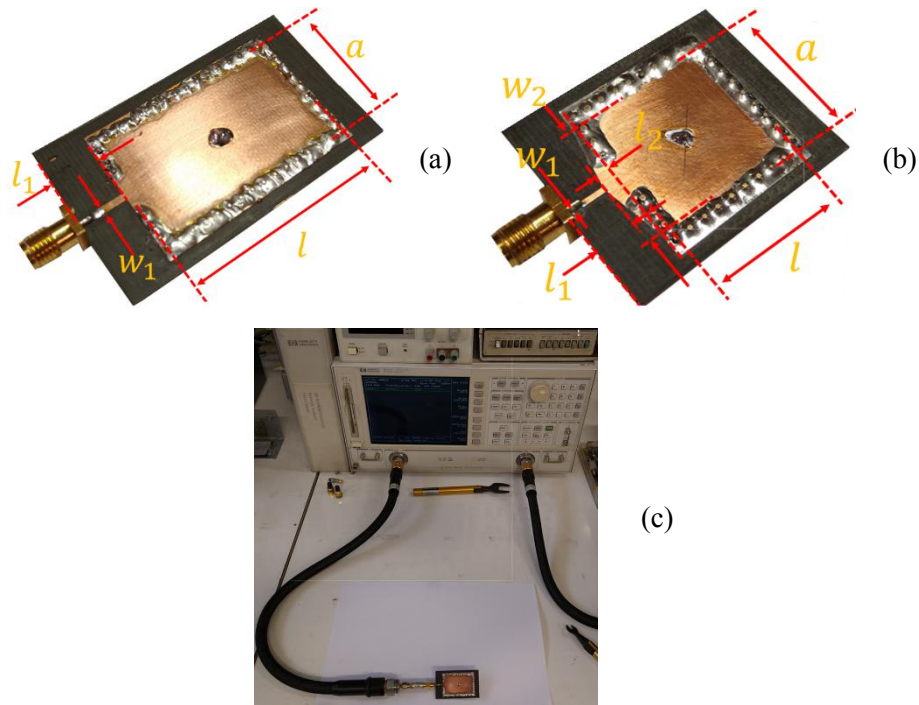


Fig. 6. (a) Rectangular cavity, (b) Square cavity, and (c) Measurement setup.

As shown in Fig. 6(a) and Fig. 6(b), both cavities are fed by a  $50 \Omega$  microstrip line, and the impedance matching of the square cavity was performed by a tapered line. For the rectangular cavity, was not required an impedance network due to the good impedance match provided by the fed line over the considered bandwidth. According to Fig. 6(a), the physical dimensions of the rectangular cavity are:  $l_1 = 8.50$  mm,  $w_1 = 1.40$  mm,  $l = 39.0$  mm,  $a = 24.2$  mm, and  $d_p = 1.20$  mm. According to Fig. 6(b), the physical dimensions of the square cavity are:  $l_1 = 6.00$  mm,  $w_1 = 1.40$  mm,  $l_2 = 2.00$  mm,  $w_2 = 21.0$  mm,  $l = 24.2$  mm,  $a = 24.2$  mm, and  $d_p = 0.8$  mm. Regarding the fabrication process, the SIW sidewalls were implemented using pins of low-cost pin-head connectors, copper conductors, with a longitudinal spacing  $p$  of 2.54 mm.

Concerning the electrical characterization, two steps were considered: the first step was the original cavity, without perturbation, and the second step was the cavity perturbed by a change in shape. For the perturbed cavity, the dielectric substrate was drilled, and the metal post was soldered at the bottom and upper walls. Fig. 7 shows the frequency response of both resonant cavities.

The frequency response of the rectangular cavity is presented in Fig. 7(a). Concerning simulation results, Fig. 7(a) shows a  $|S_{11}|$  of 14.87 dB at  $f_o$  of 4.98 GHz with an error of 0.40%, and  $|S_{11}|$  of 10.68 dB at  $f_p$  of 5.93 GHz with an error of 1.17%. Regarding experimental results, Fig. 7(a) shows a  $|S_{11}|$  of 11.21 dB at  $f_o$  of 4.96 GHz with an error of 0.80%, and  $|S_{11}|$  of 9.31 dB at  $f_p$  of 5.84 GHz with an error of 2.67%. It is important to note that for  $0 \leq \delta \leq 0.50$  or  $0.50 \leq \delta \leq 1$ , the perturbed resonance frequency varies in the frequency range  $4.96 \text{ GHz} \leq f_p \leq 5.84 \text{ GHz}$ .

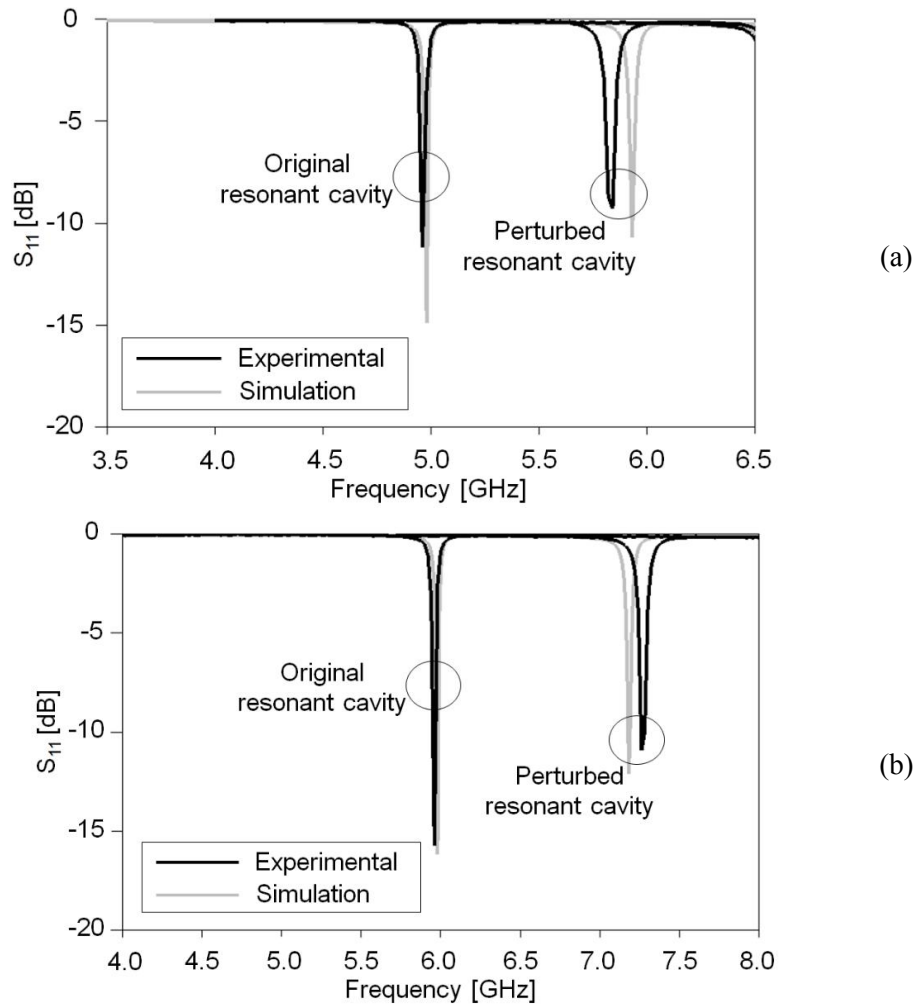


Fig. 7. (a) Frequency response of the rectangular cavity and (b) Frequency response of the square cavity.

The frequency response of the square cavity is presented in Fig. 7(b). Concerning simulation results, Fig. 7(b) shows a  $|S_{11}|$  of 16.16 dB at  $f_o$  of 5.98 GHz with an error of 0.33%, and  $|S_{11}|$  of 12.10 dB at  $f_p$  of 7.18 GHz with an error of 0.28%. Regarding experimental results, Fig. 7(b) shows a  $|S_{11}|$  of 15.74 dB at  $f_o$  of 5.96 GHz with an error of 0.67%, and  $|S_{11}|$  of 10.93 dB at  $f_p$  of 7.26 GHz with an error of 0.83%. For  $0 \leq \delta \leq 0.50$  or  $0.50 \leq \delta \leq 1$ , the perturbed resonance frequency varies in the frequency range  $5.96 \text{ GHz} \leq f_p \leq 7.26 \text{ GHz}$ .

The experimental results show that the resonance frequencies were tuned by 17.74% and 21.81% for the rectangular and square cavities, respectively. These frequency variations are compatible with the 20% for  $\delta = 0.50$  predicted by (14). Still regarding the experimental results, was verified an arithmetic mean error of 1.75% for the predicted  $f_p$ , validating the proposed design procedure. In many practical applications, microwave switches can provide electronic and mechanical frequency tuning [10],[12]-[16], however, the tuning range is reduced by the no-ideal behavior and parasitic effects [10],[16]. Thus, the experimental resonance frequency value will be lower than the one

predicted by (14). Aiming to compare this work with other previous works, a performance summary is presented in Table I.

TABLE I. PERFORMANCE SUMMARY AND COMPARISON WITH OTHER PUBLISHED WORKS.

Reference	Prototype or Structure in SIW technology	Metal posts inserted	$f_o$ [GHz]	$\Delta f$ [%]	Did the work present an equation to predict the perturbed resonance frequency?	Did the work consider the position variation of the metal post in the investigation?	Did the work consider the physical dimensions variation of the metal post in the investigation?
[13]	Two-pole bandpass filter	4	1.55	+29	No	Yes	No
[10]	Square resonant cavity	1	3.40	+18	Yes	No	No
This work	Rectangular resonant cavity	1	4.96	+17.74	Yes	Yes	Yes
	Square resonant cavity	1	5.96	+20.81			
[11]	First demonstrator	1	9.97	-5.3	No	No	No

According to the published works presented in Table I, the novel design procedure allowed a frequency variation ( $\Delta f$ ) up to 20% employing only one metal post. Generally, to obtain a  $\Delta f$  about 20% is used more than one metal post which leads to an increase in the manufacturing cost due to the use of microwave switches and biasing networks. It is important to note that the use of various microwave switches to connect and disconnect the upper and bottom walls of the cavity reduces the frequency tuning and deteriorates the frequency response. Since an open metal post into the cavity does not significantly change its field distributions [10],[16]-[17], two or more metal posts can be used to achieve different operation states using the proposed design procedure, connecting and disconnecting the upper and the bottom walls, allowing various states in the frequency range  $f_o \leq f_p \leq 1.2f_o$ . Moreover, this work is the first one that presents an investigation proposing an equation to predict the perturbed resonance frequency as a function of the position and considering the physical dimensions of the metal post.

#### IV. CONCLUSION

A design procedure employing a novelty developed in this work and named as Perturbation Factor is presented to predict the resonance frequency of resonant cavities in SIW technology perturbed by a single metal post inserted in its internal volume, connecting the bottom and upper metal walls. Another novelty is that the physical dimensions of the metal post were also considered during the investigation. Due to the equivalence of operation between rectangular waveguide resonators and

resonant cavities in SIW technology, the novel design procedure can be applied in filters with shunt reactance of symmetrical inductive window and tunable cavities. Its application is straightforward and allows a particularly good frequency variation, up to 20%, using only one metal post and reducing the fabrication cost.

#### ACKNOWLEDGMENT

The authors would like to acknowledge the Rogers Corporation for providing the substrate samples.

#### REFERENCES

- [1] J. Lee, E. Tejedor, K. Ranta-aho, *et al.*, “Spectrum for 5G: Global Status, Challenges, and Enabling Technologies”, *IEEE Commun. Mag.*, vol. 56, no. 3, pp. 12–18, 2018.
- [2] E. Doumanis, G. Goussetis, J. Vuorio, *et al.*, “Tunable Filters for Agile 5G New Radio Base Transceivers Stations”, *IEEE Microw. Mag.*, vol. 22, no. 11, pp. 26–37, 2021.
- [3] X. Chen, K. Wu, “Substrate Integrated Waveguide Filter: Basic Design Rules and Fundamental Structure Features”, *IEEE Microw. Mag.*, vol. 15, no. 5, pp. 108–116, 2014.
- [4] M. Bozzi, A. Georgiadis, K. Wu, “Review of substrate-integrated waveguide circuits and antennas”, *IET Microw., Antennas Propag.*, vol. 5, no. 8, pp. 909–920, 2011.
- [5] F. Xu, K. Wu, “Guided-wave and leakage characteristics of substrate integrated waveguide”, *IEEE Trans. Microw. Theory Techn.*, vol. 53, no. 1, pp. 66–73, 2005.
- [6] Y. Cassivi, L. Perregini, P. Arcioni, *et al.*, “Dispersion Characteristics of Substrate Integrated Rectangular Waveguides”, *IEEE Microw. Compon. Lett.*, vol. 12, no. 9, pp. 333–335, 2002.
- [7] D. Deslandes, K. Wu, “Accurate Modeling, Wave Mechanisms, and Design Considerations of a Substrate Integrated Waveguide”, *IEEE Trans. Microw. Theory Techn.*, vol. 54, no. 6, pp. 2516–2526, 2006.
- [8] M. Bozzi, L. Perregini, K. We, “Modeling of Conductor, Dielectric, and Radiation Losses in Substrate Integrated Waveguide by Boundary Integral-Resonant Mode and to Method”, *IEEE Trans. Microw. Theory Techn.*, vol. 56, no. 12, pp. 3153–3161, 2008.
- [9] R. C. Caleffo, F. S. Correra, “Liquids electrical characterization sensor using a hybrid SIW resonant cavity”, *Microw Opt Technol Lett.*, vol. 60, no. 2, pp. 445–449, 2018.
- [10] R. C. Caleffo, F. S. Correra, “3.4/4.0 GHz tunable resonant cavity in SIW technology using metal post and PIN diode on a low-cost biasing network for 5G applications”, *J. of Microw., Optoelectronics and Electromagn. Appl.*, vol. 19, no. 1, pp. 94–105, 2020.
- [11] J. C. Bohorquez, B. Potelon, C. Person, *et al.*, “Reconfigurable Planar SIW Cavity Resonator and Filter”, *IEEE MTT-S Int. Microw. Symp. Dig.*, San Francisco, USA, pp. 947–950, 2006.
- [12] R. C. Caleffo, F. S. Correra, “A novel and compact 3.5 GHz tunable bandpass filter in SIW technology with shunt-inductive discontinuities switched by pin diode switches”, *Microw. Opt. Technol Lett.* vol. 63, no. 2, pp. 471–479, 2021.
- [13] M. Armendariz, V. Sekar, K. Entesari, “Tunable SIW Bandpass Filters with PIN Diodes”, *Eur. Microw. Conf.*, Paris, France, pp. 830–833, 2010.
- [14] K. Entesari, A. P. Saghati, V. Sekar, *et al.*, “Tunable SIW Structures: Antennas, VCOs, and Filters”, *IEEE Microw. Mag.* vol. 16, no. 5, pp. 34–54, 2015.
- [15] V. Sekar, M. Armendariz, K. Entesari, “A 1.2–1.6 GHz Substrate-Integrated-Waveguide RF MEMS Tunable Filter”, *IEEE Trans. Microw. Theory Techn.*, vol. 59, no. 4, pp. 866–876, 2011.
- [16] D. M. Pozar, *Microwave Engineering*, 4th ed. New York, NY, USA: John Wiley & Sons, Inc., 2011.
- [17] S. Ramo, J. R. Whinnery, T. V. Duzer, *Fields and waves in communication electronics*, 3rd ed. New York, NY, USA: John Wiley & Sons, Inc., 1993.
- [18] M. N. O. Sadiku, *Numerical Techniques in Electromagnetics*, 2nd. ed, Boca Raton, FL, USA: CRC Press, 2001.
- [19] M. Rezaee, A. R. Attari, “Analytical Calculation of the Resonant Frequencies for a Corner Cut Square SIW Cavity”, *Iranian Conf. on Elect. Eng.*, Shiraz, Iran, pp. 517–520, 2016.
- [20] X. Wang, D. Zhang, Q. Liu, *et al.*, “Tunable bandpass filter with wide tuning range of center frequency and bandwidth based on circular SIW”, *Int. J. Electron. Commun (AEÜ)*. vol. 114, no. 153002, pp. 1–5, 2020.
- [21] P. Liu, Z. Li, W. Fu, *et al.*, “Complementary Split-Ring Resonators in Microwave Filters: A Review and Focus on Structural Progress”, *IEEE Microw. Mag.*, vol. 23, no. 9, pp. 70–84, 2022.
- [22] E. S. S. Silveira, F. Antreich, D. C. Nascimento, “Frequency-reconfigurable SIW microstrip antenna”, *Int. J. Electron. Commun (AEÜ)*. vol. 124, no. 153333, pp. 1–9, 2020.